Journal of Organometallic Chemistry 694 (2009) 959–967

Contents lists available at ScienceDirect

Journal of Organometallic Chemistry

journal homepage: www.elsevier.com/locate/jorganchem

Glycal–ruthenium carbonyl clusters: Syntheses, characterization, and anticancer activity

V.D. Reddy [a,*], Divya Dayal [b], Stephen C. Cosenza [c], M.V. Ramana Reddy [c], William C. Pearl Jr. [d], Richard D. Adams [d]

[a] Department of Physical Sciences, Kingsborough College of The City University of New York, 2001 Oriental Blvd., Brooklyn, NY 11235, United States
[b] Stuyvesant High School, 345 Chambers Street, New York, NY 10282, United States
[c] Fels Institute for Cancer Research, Temple University School of Medicine, 3307 North Broad Street, Philadelphia, PA 19140, United States
[d] Department of Chemistry and Biochemistry, University of South Carolina, Columbia, SC 29208, United States

ARTICLE INFO

Article history:
Received 30 September 2008
Received in revised form 8 November 2008
Accepted 10 November 2008
Available online 21 November 2008

Keywords:
Anticancer agents
Glycal
Ruthenium
Bioorganometallic chemistry
Hydride ligands

ABSTRACT

Four new chiral ruthenium carbonyl cluster complexes $Ru_3(\mu\text{-}H)_2(CO)_9$(L-2H) (**1**), $Ru_3(\mu\text{-}H)_2(CO)_7$-(L-2H)(dppm) (**2**), $Ru_3(\mu\text{-}H)_2(CO)_7$(L-2H)$(PPh_3)_2$ (**3**), $Ru_3(\mu\text{-}H)_2(CO)_7$(L-2H)(dppe) (**4**) containing a dehydrogenated form (L-2H) of 3,4,6-tri-*O*-benzyl-D-galactal (L) as a chiral ligand have been prepared and characterized. The anticancer activity of five compounds **1–4** and $Ru_3(\mu\text{-}H)_2(CO)_9$(L-2H) **5** (L = tribenzyl glucal) against six types of human cancer cell lines was studied and compared to cisplatin. Compound **1** was chosen to produce more detailed growth curves based on overall highest activity profile. The structure of compound **2** was established by a single-crystal X-ray diffraction analysis. The structure based on triangular metal framework contains a bridging dehydrogenated tribenzyl galactal ligand bonded in a parallel μ_3-η^2-bonding mode and a bridging dppm ligand. Variable-temperature NMR studies show that the two hydride ligands in compounds **1** and **2** are dynamically active on the NMR time scale at room temperature.

© 2008 Elsevier B.V. All rights reserved.

1. Introduction

Cisplatin [1a] and Taxol [1b] are widely used anticancer drugs in the treatment of various cancer types. Cisplatin and Taxol exhibit a high general toxicity leading to undesirable side effects, and are inactive against certain type of cancers. There has been great interest in the syntheses of organometallic compounds in medicine [2] and also in the use of intact metal carbonyl clusters in catalysis [3]. Rosenberg and coworkers have studied the interactions of benzoheterocycle triosmium carbonyl clusters with DNA [4]. Synthesis and biochemical assay of ferrocenyl and triosmium carbonyl cluster derivatives of tamoxifen increases lipophilicity dramatically and reduces affinity for the estrogen receptor [5]. Meggers and his coworkers have shown the feasibility of organometallic ruthenium-based protein kinase inhibitors, using chiral ruthenium moieties surrounded by stable inert ligands as a spatial replacement for the carbohydrate moiety that is difficult to synthesize [6]. Carbohydrates have been shown to play a central role in a variety of significant biological events, including inflammation, metastases, immune response, and bacterial and viral infection [7]. Inhibitors of glycosidase are regarded as potential antiviral, antibacterial, antitumor, and immunomodulatory agents [8]. The synthesis of ruthenium carbonyl clusters containing 3,4,6-tri-*O*-benzyl-D-glucal (tribenzyl glucal) as a chiral carbohydrate ligand has been a major focus of attention in our laboratories [9]. The anticancer activity of the ruthenium carbonyl cluster complexes containing tribenzyl glucal ligand has prompted us to investigate the chemistry of ruthenium carbonyl clusters containing 3,4,6-tri-*O*-benzyl-D-galactal [10]. Herein we report the synthesis of ruthenium carbonyl cluster complexes $Ru_3(\mu\text{-}H)_2(CO)_9$(L-2H) (**1**), $Ru_3(\mu\text{-}H)_2(CO)_7$(L-2H)(dppm) **(2),** $Ru_3(\mu\text{-}H)_2(CO)_7$(L-2H)$(PPh_3)_2$ **(3),** $Ru_3(\mu\text{-}H)_2(CO)_7$(L-2H)(dppe) (**4**), L = 3,4,6-tri-*O*-benzyl-D-galactal (L), and $Ru_3(\mu\text{-}H)_2(CO)_9$(L-2H) (**5**) (L = tribenzyl glucal) and a first assessment of their anticancer activity**.** The chemistry of compound **1** is slightly different from **5**, the 4-*O*-benzyl group in tribenzyl galactal is in axial position as opposed to equatorial in tribenzyl glucal. This difference is noted in the higher activity of **1** versus **5** against several different types of human cancer cell lines.

2. Results and discussion

Tribenzyl galactal reacts with $Ru_3(CO)_{12}$ in benzene at reflux temperature to give the orange semi-solid 1 that has been characterized by a combination of FT-IR and NMR spectroscopy, mass spectrometry, and elemental analysis. The proposed structure for **1** is shown in Scheme 1. In the formation of **1** the two hydrogen

* Corresponding author.
E-mail address: vreddy@kingsborough.edu (V.D. Reddy).

0022-328X/$ - see front matter © 2008 Elsevier B.V. All rights reserved.
doi:10.1016/j.jorganchem.2008.11.025

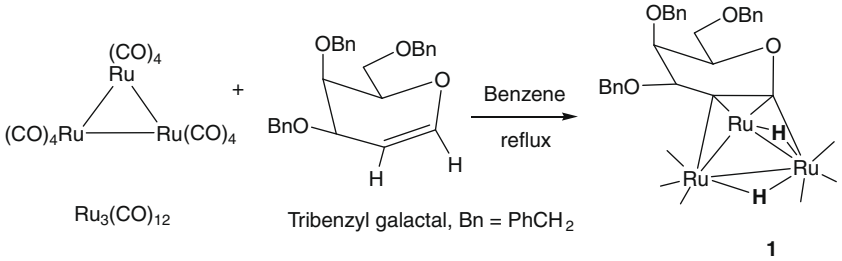

Scheme 1. Synthesis of compound **1**.

atoms on the olefinic group of the tribenzyl galactal molecule were cleaved from their carbon atoms to form the ligand tribenzyl galactal-2H, L-2H. The two hydrogen atoms were transferred to the metal atoms to become hydrido ligands. The L-2H ligand formally contains a C–C triple bond between the two dehydrogenated carbon atoms. This C–C triple bond grouping is coordinated to the triangular cluster of the three-ruthenium atoms. The proposed structure is supported by an X-ray crystal structure analysis of compound **2,** a dppm-derivative of 1 that is described below. The IR spectrum of **1** in dichloromethane exhibits stretching vibrations in the terminal carbonyl region: 2105 (m), 2078(s), 2054(s), 2030(s), 2011(s, sh) cm^{-1}. The stretching frequency at 3052 (m) is due to aromatic C–H and frequencies at 2958 (w), 2858 (w) are due to aliphatic C–H. The frequencies at 1111(m, br), 1058(m) and 1028(m) cm^{-1} are due to C–O stretching of benzyloxy groups in tribenzyl galactal. ^1H NMR spectrum of **1** in CD_2Cl_2 shows all of the hydrogens of tribenzyl galactal in the organic region: multiplet at δ 7.41–7.23 corresponding three phenyl groups, multiplet at δ = 4.92–4.48 for three methylene protons of benzyl groups, a pseudo quartet δ = 4.45 due to H-5 proton, a broad peak at δ 4.36 due to H-3 proton, a multiplet at δ = 4.36 due to H-4 proton, and a broad doublet at 3.73 which is actually doublet of doublet due to H-6 methylene protons and the two hydrogens each on C-1 and C-2 carbons were found in the hydride region as a broad resonance at δ = −18.33. At room temperature these two bridging hydride ligands rapidly exchange on the NMR time scale over all three edges of the triruthenium skeleton producing a broad resonance. The C-1 and C-2 carbons of the L-2H ligand are bonded to two-ruthenium atoms of $Ru_3(CO)_9$ framework as in $Ru_3(\mu\text{-}H)_2(CO)_9$(L-2H) (5) (L = tribenzyl glucal) in μ_3-η^2-bonding mode [9,11]. The broad resonance at δ = −18.33 in the ^1H NMR spectrum can be assigned to the two bridging hydride ligands that migrate over all three edges of the triruthenium framework in a fluxional process that is rapid on the NMR timescale at room temperature. The dynamics of this process were confirmed by a variable-temperature ^1H NMR spectroscopy. The VT-^1H NMR spectra of compound **1** in CD_2Cl_2 are available in the Supplementary material accompanying this report. At −80 °C, the broad resonance observed at room temperature has resolved into two sharp singlets at δ = −16.24 and −20.32 that have equal intensity. The singlet at δ = −20.32 can be assigned to the bridging hydrido ligand between the two-ruthenium atoms that are σ-bonded to the L-2H ligand. The other singlet at δ = −16.24 is due to the bridging hydride between the ruthenium atom bonded to the double bond and the other ruthenium atom sigma bonded to the L-2H ligand. The two singlets become featureless at about −4 °C; above −4 °C, the two resonances coalesce to one broad peak. The ^{13}C NMR spectrum of **1** at room temperature in $CDCl_3$ shows resonances for both aliphatic and aromatic regions of L-2H ligand, and resonances due to carbonyl groups: four sharp resonances of higher intensity at δ = 207.40, 197.96, 192.15, 186.52 and three broad resonances of lower intensity at 204.43, 193.58, 190.91 are due to nine carbonyl groups bonded to triruthenium atoms. The four sharp and three broad resonances indicate that the carbonyl groups undergo various stages of dynamical exchange: (a) a low energy axial–radial exchange of carbonyls on each ruthenium atom and (b) intermetallic scrambling of CO groups combined with slow oscillatory motion of L-2H ligand together with hydride migrations around the triruthenium triangle [12a–f]. The FAB+ mass spectrum shows the molecular ion peak at 972 and the successive loss of nine carbonyl groups. The isotopic distribution pattern is consistent with the presence of three-ruthenium atoms.

Compound **1** contains 48 valence electrons at the metal atoms with L-2H donating 4 electrons, the nine CO groups contribute 18 electrons, the two bridging hydride ligands contribute 2 electrons, and the three-ruthenium atoms contribute a total of 24 electrons. 48 is the number expected for trinuclear cluster containing three metal–metal bonds.

In order to facilitate crystal growth for crystallographic characterization, the yellow compound $Ru_3(CO)_7$(dppm)(L-2H), **2**, was prepared by the reaction of **1**, with 1,1-bis-(diphenylphosphino)methane, dppm, in dichloromethane solvent at room temperature by using $Me_3NO \cdot 2H_2O$ to assist in the removal of two of the CO ligands, see Scheme 2.

Compound **2** was isolated in pure form by flash column chromatography on silica gel with a hexanes/dichloromethane solvent mixture and was characterized by a combination of IR, ^1H, ^{31}P and ^{13}C NMR, mass spectrometry, elemental analysis, and single-crystal X-ray diffraction analyses.

An ORTEP diagram of the molecular structure of **2** is shown in Fig. 1. Selected bond distances and angles are given in Table 1. The molecule contains a triangular cluster of three-ruthenium atoms with a dehydrogenated triply bridging tribenzyl galactal ligand L-2H. L-2H is coordinated to the three-ruthenium atoms by two of its carbon atoms in the parallel μ_3-η^2-bonding mode, C(2) is σ-bonded to Ru(2), Ru(2)–C(2) = 2.085(5) Å and C(3) is σ-bonded to Ru(3), Ru(3)–C(3) = 2.071(5) Å. C(2) and C(3) are π-bonded to Ru(1), Ru(1)–C(2) = 2.303(5) Å and Ru(1)–C(3) = 2.290(5) Å. The C(2)–C(3) bond length of 1.377(6) Å is slightly longer than a typical carbon-carbon double bond (1.33 Å) because of its coordination to the metal atoms. The two hydrido ligands bridge the Ru(1)–Ru(2) and Ru(2)–Ru(3) bonds. As expected [13], these Ru–Ru bonds are slightly longer, 2.8459(5) Å and 2.9878(5) Å, than the Ru–Ru bond that does not have a bridging hydrido ligand, Ru(1)–Ru(3) = 2.7135(6) Å. The two hydrido ligands were located and refined in the analysis; one hydride bridges the Ru(1)–Ru(2) bond, Ru(1)–H(1) 1.748(10) Å, Ru(2)–H(1) 1.745(10) Å and the other bridges the Ru(2)–Ru(3) bond, Ru(2)–H(2) 1.67(8) Å, Ru(3)–H(2) 1.76(8) Å. The diphosphine ligand, dppm, bridges the Ru(1)–Ru(2) bond, Ru(1)–P(1) = 2.3727(13) Å and Ru(2)–P(2) = 2.3285(12) Å. Each of the phosphorus-substituted ruthenium atom contains two additional terminal carbonyl ligands, whereas the third ruthenium atom has three. A bridging hydrido ligand was found on one of the dppm-bridged Ru–Ru bonds in the cationic cluster complex $[Ru_3(\mu\text{-}H)(CO)_6(\mu\text{-dppm})_3]^+$ [14].

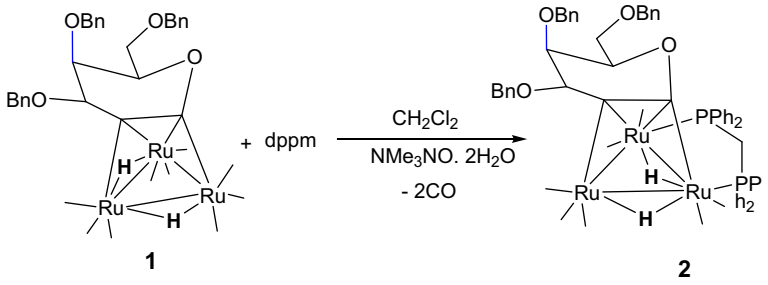

Scheme 2. Synthesis of compound **2.**

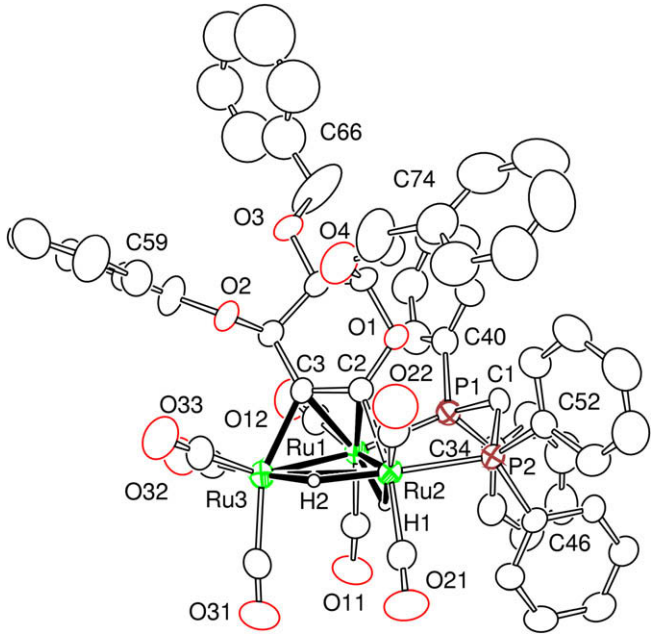

Fig. 1. ORTEP diagram of **2** showing 40% probability thermal ellipsoids. Hydrogen atoms have been omitted for clarity.

Table 1
Selected intramolecular distances and angles for $Ru_3(\mu\text{-}H)_2(CO)_7$(L-2H)(dppm) (**2**).

Atom	Atom	Distance (Å)	Atom	Atom	Distance (Å)
(a) Distances					
Ru(1)	Ru(3)	2.7135(6)	P(1)	C(1)	1.839(5)
Ru(1)	Ru(2)	2.8459(5)	P(2)	C(1)	1.832(5)
Ru(2)	Ru(3)	2.9878(5)	C(2)	C(3)	1.377(6)
Ru(1)	P(1)	2.3727(13)	C(3)	C(4)	1.521(6)
Ru(2)	P(2)	2.3285(12)	C(4)	C(5)	1.528(7)
Ru(1)	H(1)	1.748(10)	O(1)	C(2)	1.402(6)
Ru(2)	H(1)	1.745(10)	O(1)	C(6)	1.452(6)
Ru(2)	H(2)	1.67(8)	Ru(3)	C(3)	2.071(5)
Ru(3)	H(2)	1.76(8)	Ru(2)	C(2)	2.085(5)
Ru(1)	C(2)	2.303(5)			
Ru(1)	C(3)	2.290(5)			
Atom–atom–atom		Angle (°)	Atom–atom–atom		Angle (°)
(a) Angles					
Ru(1)–Ru(2)–Ru(3)		55.374(13)	P(2)–Ru(2)–Ru(1)		90.70(4)
Ru(1)–Ru(3)–Ru(2)		59.660(13)	P(2)–C(1)–P(1)		114.5(2)
Ru(3)–Ru(1)–Ru(2)		64.966(15)	Ru(2)–C(2)–Ru(1)		80.71(16)
P(1)–Ru(1)–Ru(2)		93.93(4)	Ru(3)–C(3)–Ru(1)		76.76(15)

The IR spectrum of **2** shows terminal carbonyl stretching absorptions: 2059 (s), 2031(m), 2044(m), 1993 (vs, sh), 1937(w) cm^{-1} and C–O stretching due to benzyloxy at 1096 (w, br) cm^{-1}. The ^1H NMR spectrum **2** shows a multiplet at $\delta = 7.67$–7.10 for the seven phenyl groups (three phenyl groups of the L-2H ligand and four phenyl groups from dppm), resonances at $\delta = 4.70$–3.80 due to aliphatic region of tribenzyl galactal. The multiplet at $\delta = 3.69$ and a quartet at $\delta = 3.54$ are due to the inequivalent methylene protons on the CH_2 group that links the two phosphorus atoms. There is a single broad resonance at $\delta = -17.73$ for the hydrido ligands at room temperature. However, the structural analysis shows that the two bridging hydrido ligands are inequivalent. Thus, dynamical averaging was suspected. This was confirmed by recording variable-temperature ^1H NMR spectra of compound **2**. These spectra are shown in Fig. 2. At −80 °C, the spectrum shows a doublet at $\delta = -16.07$ and a triplet at −20.38. The J_{P-H} coupling constants measured in the hydride resonances clearly indicate that the triplet with ($^2J_{P-H} = 16$ Hz) is typical of *cis* coupling corresponds to the hydride H(1) that spans the Ru(1)–Ru(2) edge of the cluster that contains the bridging dppm ligand. The doublet with ($^2J_{P-H} = 35$ Hz) is typical of *trans* coupling and corresponds to the other hydride ligand H(2) *trans* to one ^{31}P atom [15,16]. As the temperature is raised above −80 °C, the resonances broaden and merge into the single broad resonance observed at 20 °C. An intramolecular migratory exchange mechanism is proposed to explain the averaging process, see Scheme 3.

The ^{13}C NMR spectrum of **2** in CD_2Cl_2 at room temperature shows four broad resonances at δ 203.81, 202.24, 198.07,196.63 (d, $^2J_{C-P} = 9.2$ Hz) due to the seven carbonyl groups bonded to three-ruthenium atoms. The broadness of the resonances is indicative of dynamical activity of the CO ligands. The dynamical process is due to localized turnstile rotations of the carbonyl ligands (phosphine substitution appears to raise the barrier for axial-radial exchange) followed by intermetallic CO scrambling that combine with an oscillatory motion of L-2H ligand and hydride migrations [12a,b]. At −80 °C ^{13}C NMR shows in the carbonyl region six resonances for seven carbonyl groups at $\delta = 209.19$, 205.79 (2CO), 199.90, 198.98, 193.54, 190.00. The multiplets at $\delta = 138.92$–126.73 are due to C-1 carbon, the three phenyl groups of tribenzyl galactal-2H ligand, and the four phenyl groups of a dppm ligand. The resonances at $\delta = 110.97$ (d, $^2J_{C-P} = 8.5$ Hz) are corresponding to C-2 carbon, peaks at $\delta = 80.00$, 79.15, 74.99, 73.71, 69.83, 69.62, 69.10 due to aliphatic regions of tribenzyl galactal, and a broad peak at $\delta = 42.50$ is due to methylene carbon of the dppm ligand. The ^{13}C NMR at room temperature exhibits a triplet at $\delta = 37.52$ ($^2J_{P-H} = 21$ Hz) corresponding to methylene carbon of dppm with coupling to the two phosphorus nuclei. The ^{31}P NMR spectrum shows two broad resonances at $\delta = 27.52$ and 20.33 and sharp peak at $\delta = 23.54$ indicating that the two phosphorus atoms are inequivalent due to asymmetric ligand environment. The broad nature of the signal is due to the unresolved coupling to the dppm methylene protons and to the bridging hydride ligands [16]. The FAB+ mass spectrum shows a molecular ion peak centered at 1301. The isotopic pattern is consistent with the presence of the three-ruthenium atoms.

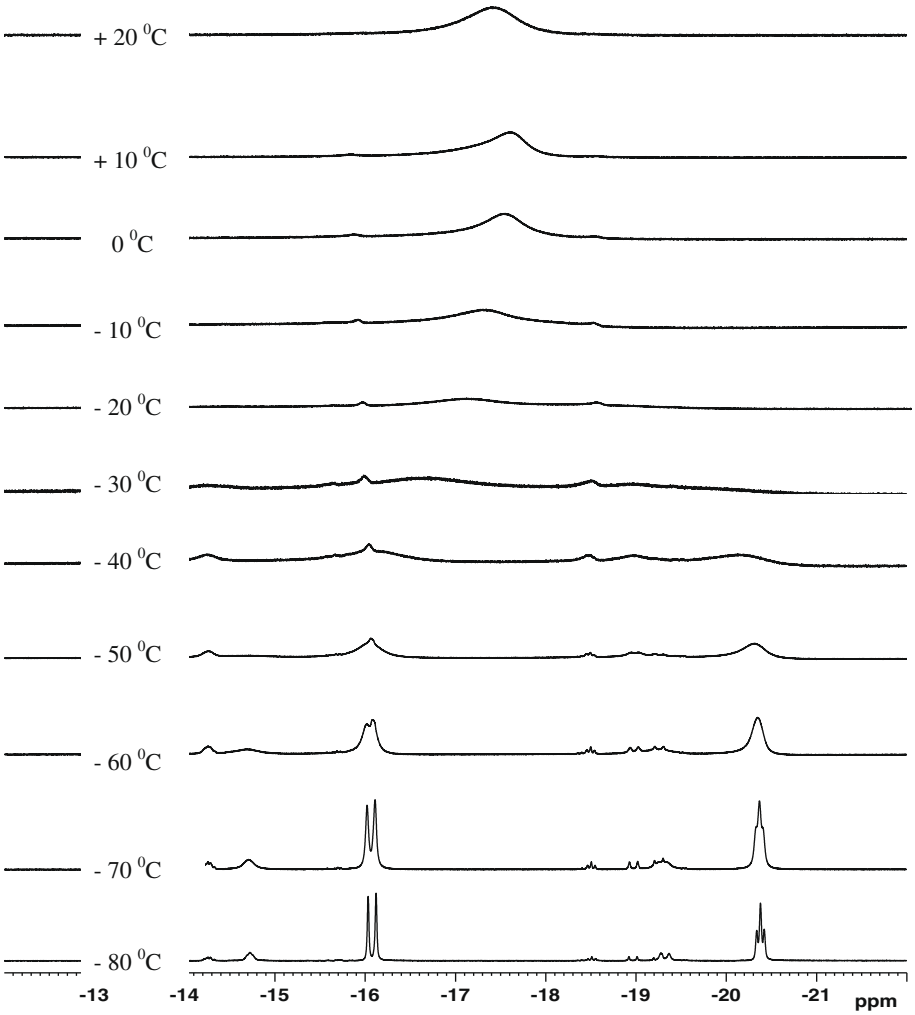

Fig. 2. Variable-temperature ^{1}H NMR spectra of compound **2** in CD_2Cl_2 in the hydride region. The small peaks are believed to be due to impurities in the sample.

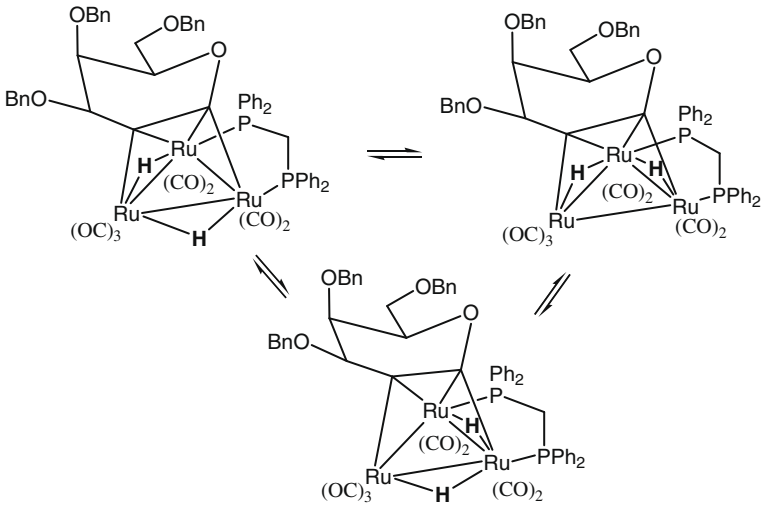

Scheme 3. An intramolecular mechanism for the exchange of the hydrido ligands in **2**.

Compound **1** also reacts with triphenylphosphine in the presence of $Me_3NO \cdot 2H_2O$ in dichloromethane to yield the new yellow cluster complex $Ru_3(\mu\text{-}H)_2(CO)_7(L\text{-}2H)(PPh_3)_2$ (**3**). Compound **3** was purified by flash column chromatography with hexanes/dichloromethane (8:2, v/v) and was characterized by IR and NMR spectroscopic data, mass spectrometry, and elemental analysis. The IR spectrum of **3** in dichloromethane exhibits stretching frequencies of the terminal carbonyl ligands at 2079 (w), 2061(s), 2044(m), 2030 (s), 1995(vs, sh), 1941(w) cm^{-1} and a C–O stretching absorption due to benzyloxy groups at 1094 (br) cm^{-1}. The ^{1}H

NMR spectrum of **3** in CD_2Cl_2 shows multiplets at $\delta = 7.9–7.1$ corresponding to the nine phenyl groups (3 phenyl groups from L-2H ligand and 6 phenyl groups from two triphenyl phosphine ligands); a multiplet at $\delta = 4.92–4.42$ for the eight hydrogen atoms (6 benzylic hydrogens of three phenyl groups in L-2H ligand, H-5, and H-4); a broad unresolved peak at δ 4.24 due to H-4; a pseudo doublet $\delta = 3.76$ is attributed to two hydrogen atoms bonded to C-6, and two hydrido ligands coupled to the phosphorus atoms in the high field region. At room temperature, three sets of signals at approximately intensity 1: 0.19: 0.08 (see Supplementary material) are observed for the hydrido ligands in the high field region of ^{1}H NMR spectrum of compound **3**. This strongly indicates that **3** exists as a mixture of isomers in solution. Proposed structures for isomers of **3** that are consistent with the spectroscopic data are shown in Scheme 4.

The first set of signals with intensity 1 is assigned to the major isomer **3a**; a virtual doublet at $\delta = -15.97$ [$^2J_{P-H} = 15.4$ Hz] is due to a hydride ligand (located between a ruthenium atom that is 'σ' bonded to the L-2H ligand and a ruthenium atom π-bonded to L-2H ligand) with coupling to a phosphorus atom and a virtual triplet which is actually a doublet of doublets at $\delta = -19.58$ [$^2J_{P-H} = 13.7$ Hz, 13.7 Hz] that is attributed to the second hydride ligand (positioned between the two-ruthenium atoms that are 'σ' bonded to the L-2H ligand) due to coupling to the two inequivalent phosphorus atoms [16,17]. The ^{13}C NMR spectrum of **3** in CD_2Cl_2 shows strong resonances in the carbonyl region at $\delta = 204.79$, 202.09, 198.42, 195.37, 194.65, 193.54, 193.34 (d, $^2J_{C-P} = 8.0$ Hz), 192.35, 188.07 due to carbonyl groups of the major isomer along with weaker resonances at $\delta = 206.67$, 197.93, 195.04,192.08, 187.91 due to carbonyl groups of the minor isomer in the mixture, multiplets at $\delta = 139.21–126.93$ due to C-1 carbon, the three phenyl groups of L-2H ligand, and the phenyl groups of a triphenylphosphine ligands. The resonances at $\delta = 110.34$, 104.56 (doublet, $^2J_{C-P} = 8.4$ Hz) correspond to the C-2 carbon atoms in the mixture, peaks at $\delta = 82.41$, 79.43, 75.51, 73.91, 73.78, 71.49, and 71.37 due to aliphatic carbon atoms of the L-2H ligand of the two isomers. The ^{31}P NMR spectrum of **3** in CD_2Cl_2 at room temperature shows singlets at $\delta = 42.04$, 41.46, 41.07, 39.99, 36.72, 36.17, 35.73, 35.04, and $\delta = 34.64$.

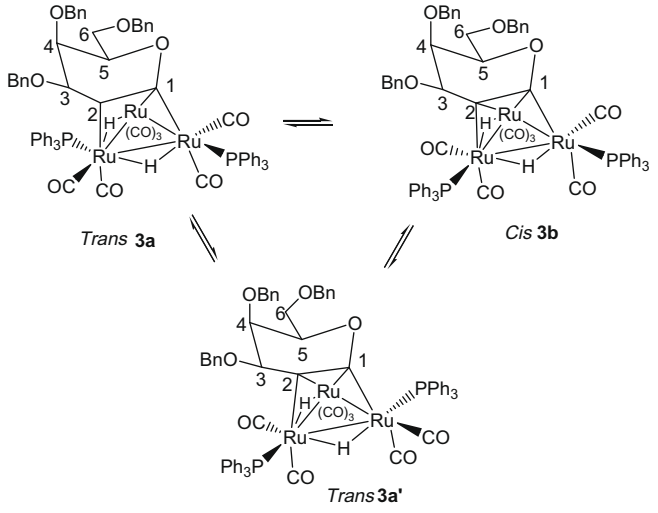

Scheme 4. Proposed structures of the isomers of compound **3** in solution.

The yellow complex **4** was obtained from the reaction of **1** with 1,2-bis(diphenylphosphino)ethane (dppe) in dichloromethane in the presence of $Me_3NO \cdot 2H_2O$ at room temperature as shown in Scheme 5.

Compound **4** was purified by flash column chromatography with hexanes/dichloromethane (8:2, v/v) and characterized by spectroscopic data, mass spectrometry, and elemental analysis. The FT-IR spectrum in dichloromethane exhibits terminal carbonyl stretching frequencies at 2061(s), 2025(s), 2000(vs), 1972(m), 1941 (w) cm^{-1} and C–O stretching due to benzyloxy at 1098 (br) cm^{-1}. The ^{1}H NMR spectrum of **4** in CD_2Cl_2 shows three multiplets at $\delta = 2.85$ (2H), 2.51 (1H) and 1.90 (1H) for the four inequivalent methylene hydrogen atoms on the dppe ligand. A multiplet at $\delta = 8.00–7.13$ due to three phenyl groups from L-2H ligand and the four phenyl groups of the dppe ligand. Resonances due to the hydrogen atoms of the L-2H appear at $\delta = 4.80–3.00$. There are two equal intensity hydride resonances: a triplet at $\delta = -20.62$ with P–H coupling, $^2J_{P-H} = 16.63$ Hz, typical of a *cis* orientation of the equivalent phosphorus atoms of the dppe ligand, and the doublet at $\delta = -16.01$ ($^2J_{P-H} = 35.95$ Hz) that is attributed to the second bridging hydride ligand which is *trans* coupled to one of the phosphorus atoms [17]. The ^{13}C NMR spectrum of **4** in CD_2Cl_2 at room temperature shows resonances at $\delta = 205.91$, 204.97 (br), 204.35, 200.19, 198.19, 193.83 (br), 193.20 (t, $^2J_{C-P} = 11.5$ Hz), 188.95 (br) are due to carbonyl groups that are broad due to dynamical activity. The chiral capping ligand makes the two faces of the ruthenium triangle inequivalent. The resonances between $\delta = 141.62–127.22$ are due to C-1 carbon, three phenyl groups of the L-2H ligand, four phenyl groups of a dppe ligand, and a doublet at $\delta = 111.82$ for C-2, ($^2J_{C-P} = 7.6$ Hz). The resonances at $\delta = 79.29$, 78.11, 73.96, 75.09, 73.86, 70.92, 69.72, 69.38 are due to aliphatic carbon atoms of the L-2H ligand, and two doublets at $\delta = 27.65$ ($^2J_{C-P} = 25.3$ Hz), δ 23.64 ($^2J_{C-P} = 31.4$ Hz) are due to methylene carbons of the dppe ligand coupling with two non-equivalent phosphorus nuclei. The ^{31}P NMR spectrum of **4** shows a virtual doublet at $\delta = 44.23$ (d, $^2J_{P-P} = 9.89$ Hz), and a broad multiplet at $\delta = 37.55$ due to two non-equivalent phosphorus atoms as a result of chiral Ru_3 framework that is asymmetric due to different ligand environment. FAB+ mass spectrum shows a molecular ion peak at 1315. The isotopic distribution pattern is consistent with the presence of three-ruthenium atoms. The spectroscopic data obtained for **4** are consistent with the structure shown in Scheme 5.

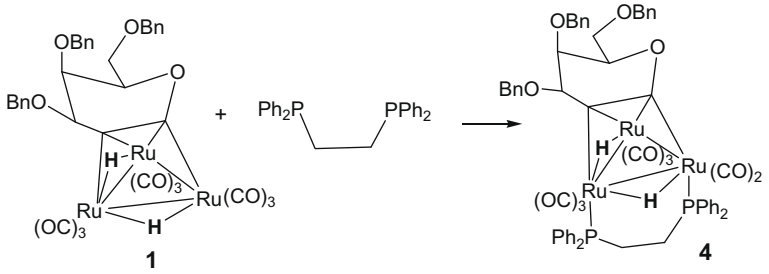

Scheme 5. Synthesis of compound **4**.

3. Anticancer activity

The *in vitro* anticancer activity of compounds **1–5** and **cisplatin** was determined using six types of human cancer cell lines: DU145 (prostate), MCF-7 (breast), SK-OV-3 (ovarian), K562 (CML: chronic myelogenous leukemia), RAJI (B-cell lymphoma), and MOLT-4 (ALL: T-cell acute lymphoblastic leukemia). Chronic myelogenous leukemia was found to be the most sensitive to all five ruthenium carbonyl clusters. Compound **1** was most active in all cell lines with over all highest activity profile with IG_{50} value of 25 μM in the B-cell lymphoma and T-cell acute lymphoblastic leukemia cancer cell lines, 30 μM in the breast, ovarian, chronic myelogenous leukemia cancer cell lines, and 40 μM in the prostate cancer cell lines (Table 2 and Fig. 3).

The activity of compound **5** is comparable to **1** in chronic myelogenous leukemia and B-cell lymphoma cancer cell lines, but it shows moderate cytotoxicity against four other cancer cell lines. This difference in activity between **1** and **5** can be attributed to the axial 4-benzyloxy group in **1** as opposed to equatorial in compound **5**. The cytotoxicity of compound **5** is quite high on chronic myelogenous leukemia (CML) and B-cell lymphoma cancer cell lines that may be due to selective binding of **5** to the leukemia cell surface receptors that involve several important signaling pathways. The substitution of two carbonyl groups in **1** with dppm, triphenyl phosphine and dppe ligands exhibit lower toxicity of the ruthenium carbonyl cluster in all tested cell lines. The in *vitro* cytotoxicity of **1** was compared to the activity of **cisplatin** (Table 3 and Fig. 4).

Table 2
GI_{50} values for compounds **1–5.**

Compound	DU145 prostate	MCF-7 breast	SK-OV-3 ovarian	K562 CML	RAJI B-cell lymphoma	MOLT-4 ALL
1	40	30	30	30	25	25
2	80	90	90	75	75	70
3	>100	80	>100	70	70	70
4	>100	80	80	40	70	60
5	80	80	75	25	25	60

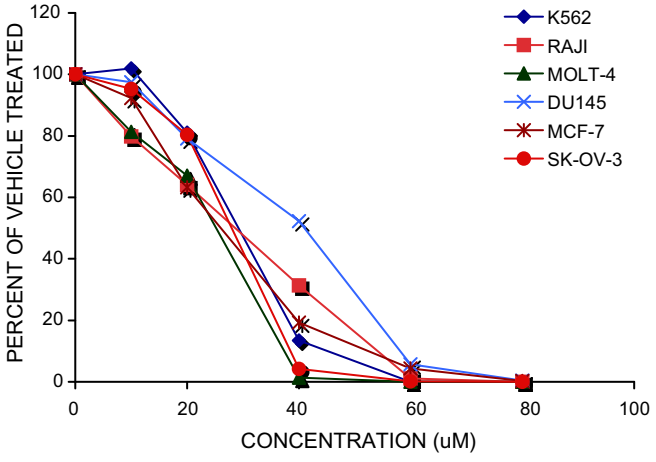

Fig. 3. Compound **1** dosage response assay.

Table 3
GI_{50} values of compound **1** and **cisplatin**.

Cell line	Tumor type	**1** (μM)	Cisplatin (μM)
DU145	Prostate	40	1.5
MCF-7	Breast	30	2.5
MCF-7	Breast	30	2.5
SK-OV-3	Ovarian	30	0.75
K562	CML	30	2.5
RAJI	B-cell lymphoma	25	2.0
MOLT-4	ALL	25	0.75

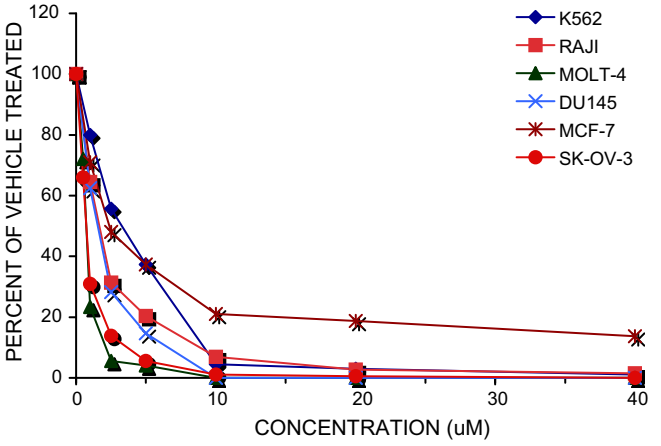

Fig. 4. Cisplatin dosage response assay.

4. Conclusions

Chiral ruthenium carbonyl clusters containing glycals have been synthesized and evaluated for potential anticancer activity. Chronic myelogenous leukemia was found to be the most sensitive to all five glycal–ruthenium carbonyl clusters. Compound **1** was most active in all cell lines with highest activity profile overall, and it compared favorably to the activity of cisplatin. Substitution of two carbonyl ligands by phosphine ligands lowers the activity relative to **1**. At present, we are pursuing synthetic studies aimed at replacing carbonyl ligands with other ligands and also fine-tuning the glycal moiety to improve the anticancer activity.

5. Experimental

5.1. General procedures

All operations were carried out under pure argon or nitrogen with the use of Schlenk techniques. The solvents were purified and distilled under an argon or nitrogen atmosphere. Flash column chromatography was performed on silica gel 60 (200–400) using the indicated solvent. Thin layer chromatography was carried out using silica gel plates with plastic backs. Infrared spectra were recorded on a Nicolet Impact 400 FT-IR spectrometer as dichloromethane solution in 0.1 mm path length NaCl cells, ^{1}H NMR spectra were recorded at 400 MHz, and Carbon-13 nuclear magnetic resonance (^{13}C NMR) spectra were recorded at 100 MHz. NMR Spectra were recorded in CD_2Cl_2, $CDCl_3$ and referenced either to internal TMS or the residual solvent peak. The ^{31}P (162 MHz) chemical shifts reported based on an internal calculation using the solvent lock signal. FAB+ Mass spectra were recorded on a VG analytical ZAB-SE and Q-TOF Mass Spectrometers at University of California, Riverside. The observed isotopic distribution is in good agreement with the calculated ones. Elemental analysis was carried out at Quantitative Technologies Inc., New Jersey.

5.2. Synthesis of $[Ru_3(CO)_9(C_{27}H_{28}O_4)]$ (**1**)

$Ru_3(CO)_{12}$ (639.34 mg, 1.0 mmol) and tri-*O*-benzyl-D-galactal (416.12 mg, 1.0 mmol) were added to a two-necked 50-mL round

bottom flask. Ten milliliter of degassed dry benzene was added under argon atmosphere and the solution was refluxed gently for 4 days similar to the synthesis of **5** [9]. Benzene was removed in vacuo and the product was isolated by flash column chromatography. Elution with hexanes/ dichloromethane (7:3, v/v) gave an orange semi-solid (274 mg, 28%). Spectroscopic data for **1**: IR (CH_2Cl_2): C–H stretching 3052 (m), 2958 (w), 2858 (w); terminal carbonyl stretching: 2105 (m), 2078(s), 2054(s), 2030(s), 2011(s, sh); C–O stretching due to benzyloxy 1111(m, br), 1058 (m) and 1028 (m) cm^{-1}. ^1H NMR: (CD_2Cl_2): δ 7.41–7.23 (m, 15H, three phenyls), 4.92–4.48 (m, 6H, 3PhCH_2O), 4.46 (q, 1H, H-5), δ 4.45 (br, 1H, H-3), 3.91–3.73 (pseudo doublet, 3H, H-4 and two hydrogens attached to C-6), −18.31 (br, 2H). ^{13}C NMR ($CDCl_3$): δ 207.40, 204.43, 197.96, 193.58, 192.15, 190.91, 186.52 carbonyls, 137.65 (s, C-1), 138.30 (3C with no hydrogens attached in the phenyl rings), 130.18–128.15 (15C: C*H* carbons of 3 phenyl groups), 105.46 (s, C-2), 80.93, 79.25, 75.23, 74.02, 72.53, 71.40, 70.28, 68.80 (aliphatic region of tribenzyl galactal carbons). FAB+ mass spectrum: 972 $[M]^+$, 944 $[M-CO]^+$, 888 $[M-3CO]^+$, 860 $[M-4CO]^+$, 832 $[M-5CO]^+$, 804 $[M-6CO]^+$, 776 $[M-7CO]^+$, 748 $[M-8CO]^+$, and 720 $[M-9CO]^+$, 718 $[M-(9CO+2H)]^+$, 516 $[M-(9CO+2H+2Ru)]^+$, 415 $[M-(9CO+3Ru)]^+$. Anal. Calc. for $C_{36}H_{28}O_{13}Ru_3$: C, 44.49; H, 2.90. Found: C, 44.58; H, 3.01%.

5.3. Synthesis of $[Ru_3(CO)_7(dppm)(C_{27}H_{28}O_4)]$ (**2**)

To a two-necked 50 mL round bottom flask was added 5.0 mL of dry dichloromethane containing compound **1** (185.0 mg, 0.19 mmol) via syringe under nitrogen atmosphere. This was followed by the addition of solid dppm (165.0 mg, 0.43 mmol) with stirring for 5 min. To this solution $Me_3NO \cdot 2H_2O$ solid (7.5 mg, 0.067 mmol) was added and the solution was stirred at room temperature overnight. During this time the color of the solution changed from orange to red. TLC analysis indicated approximately 90% conversion to product. The dichloromethane was removed in vacuo and the product was isolated by a silica gel flash column chromatography eluting with hexanes/dichloromethane (8:2, v/v) to give a fluffy yellow compound (126 mg, 52%) and 18.0 mg of unreacted **1**. Spectroscopic data for **2**: FT-IR (CH_2Cl_2): 2059 (s), 2031(m), 2044(m), 1993 (vs, sh), 1937(w) cm^{-1} and C–O stretching due to benzyloxy at 1096 (w, br) cm^{-1}. ^1H NMR: (CD_2Cl_2) δ 7.67–7.10 (m, 35H, (3*Ph*CH_2 and *Ph*$_2$PCH$_2$P*Ph*$_2$), 4.81 (d, 1H, PhC*H*$_2$) 4.62–4.29 (4H, 2PhC*H*$_2$), 4.32–4.08 (3H, H-5, H-3, one of hydrogens from PhC*H*$_2$), 3.92–3.81 (3H, two hydrogens attached to C-6, H-4), 3.65 (m, 1H, $Ph_2PCH^aH^bPPh_2$), 3.42 (q, 1H, $Ph_2CH^aH^bPh_2$), −17.45 (s, br, 2H); ^{13}C NMR (CD_2Cl_2): at −80 °C: δ 209.19, 205.79 (2CO), 199.90, 198.98, 193.54, 190.00 due to seven carbonyl groups, 138.92–126.73 (m, C-1 carbon, 3*Ph*CH_2, *Ph*$_2$CH_2*Ph*$_2$), 110.97 (d, C-2, $^2J_{C-P}$ = 8.5 Hz), 80.00, 79.15, 74.99, 73.71, 69.83, 69.62, 69.10 (aliphatic regions of tribenzyl galactal), 42.50 ($Ph_2CH_2Ph_2$); ^{31}P NMR ($CDCl_3$): δ 27.52 (br), 20.33(br), 23.54 (s); FAB+ mass spectrum: 1301 $[M]^+$, 1217 $[M-3CO]^+$; ES+/MS *m*/*z* calcd for M+H, $[C_{59}H_{50}O_{11}P_2Ru_3+H]^+$ 1302, found 1302. Anal. Calc. for $C_{59}H_{50}O_{11}P_2Ru_3$: C, 54.50; H, 3.88. Found: C, 54.96; H, 4.08%.

5.4. Synthesis of $[Ru_3(CO)_7(PPh_3)_2(C_{27}H_{28}O_4)]$ (**3**)

To a two-necked 50 mL round bottom flask was added 5.0 mL of dry dichloromethane containing compound **1** (146.0 mg, 0.15 mmol) via syringe under nitrogen atmosphere. This was followed by solid triphenylphosphine (156.0 mg, 0.60 mmol). The solution was stirred for 5 min. To this solution $Me_3NO \cdot 2H_2O$ solid (11.6 mg, 0.1 mmol) was added. This solution was then stirred at room temperature for 5 h. During this time the color of the solution turned from orange to red. Complete consumption of compound **1** was indicated by TLC analysis. The methylene chloride solvent was then removed in vacuo and the product was isolated by flash column chromatography on silica gel. Elution with hexanes/dichloromethane (8:2, v/v) gave a yellow sticky powder (136 mg, 63%). Spectroscopic data for **3**: IR (CH_2Cl_2): 2079 (w), 2061(s), 2044(m), 2030 (s), 1995(vs, sh), 1941(w) cm^{-1} and C–O stretching due to benzyloxy at 1094 (br) cm^{-1}. ^1H NMR (CD_2Cl_2): δ 7.90–7.10 (m, 45H, 3*Ph*CH_2, 2P*Ph*$_3$), 4.92–4.42(m, 8H, 3PhC*H*$_2$, H-5, H-3), 4.24 (br, 1H, H-4), 3.78 (d, 2H, two hydrogens attached to C-6), major isomer in the hydride region: −15.97 (d, 1H, J_{H-P} = 15.4 Hz), −18.58 (dd, 1H, J_{H-P} = 14.1 Hz); ^{13}C NMR(CD_2Cl_2): δ 204.79, 202.09, 198.42, 194.65, 193.54, 193.34 (d, $^2J_{C-P}$ = 8.0 Hz), 192.35, 192.08, 188.07 (CO groups in cis/trans isomeric mixture), 139.21–126.93 (m, due C-1, 3*Ph*CH_2, 2*PPh*$_3$), 110.34, 104.56 (d, $^2J_{C-P}$ = 8.4 Hz), C-2 in the *cis*/*trans* mixture, 82.41, 79.43, 75.51, 73.91, 73.78, 71.49, 71.37 (carbons in the aliphatic regions of tribenzyl galactal in the mixture); ^{31}P NMR (CD_2Cl_2): δ 42.04, 41.46, 41.07, 39.99, 36.72, 36.17, 35.73, 35.04, 34.64 for the isomeric mixture; FAB+ mass spectrum: 1441 $[M]^+$, 1413 $[M-CO]^+$, 1357 $[M-3CO]^+$, 1329 $[M-4CO]^+$, 1301 $[M-6CO]^+$, 1038$[M-(6CO+PPh_3)]^+$, 748 $[M-\{7CO+(PPh_3)_2\}]$. Anal. Calc. for $C_{70}H_{58}O_{11}P_2Ru_3$: C, 58.37; H, 4.06. Found: C, 58.11; H, 3.84%.

5.5. Synthesis of $[Ru_3(CO)_7(dppe)(C_{27}H_{28}O_4)]$ (4)

To a two-necked 50-mL round bottom flask, 5.0 mL of dry dichloromethane containing compound **1** (107.3 mg, 0.11 mmol) was added via syringe under nitrogen atmosphere followed by solid dppe (106.3 mg, 0.267 mmol) and stirred for 5 min. To this solution was then added solid $Me_3NO \cdot 2H_2O$ (10.0 mg, 0.09 mmol). The solution was stirred at room temperature for 4 h. During this time the color of the solution turned from orange to red. Complete conversion was indicated by TLC analysis. The methylene chloride solvent was then removed in vacuo and the product was isolated by chromatographic work-up on a silica gel flash column chromatography eluting with hexanes and dichloromethane (8:2, v/v) to give a fluffy yellow of compound **4** (82 mg, 57%). Spectroscopic data for **4**: IR (CH_2Cl_2): 2061(s), 2025(s), 2000(vs), 1972 (m), 1941(w) cm^{-1}. ^1H NMR (CD_2Cl_2) δ 8.10–7.13 (m, 35H), 4.80–4.05 (m, 6H, 3PhC*H*$_2$), 4.13 (q, overlapped with other peaks1H, C-5), 3.68–3.53 (m, 2H, H-3, H-4), 3.54–3.00 (m, 2H, two hydrogens attached to C-6 carbon), 2.92–2.72 (m, 2H, $Ph_2PCH_2CH_2PPh_2$), 2.60–2.47 (m, 1H, $Ph_2PCH_2CH_2PPh_2$), δ 1.98–1.82 (m, 1H, $Ph_2PCH_2CH_2PPh_2$), −16.01 (d, 1H, $^2J_{P-H}$ = 35.95 Hz), −20.62 (t, $^2J_{P-H}$ = 16.63 Hz); ^{13}C NMR (CD_2Cl_2): δ 205.91, 204.97, 204.35, 200.19, 198.19, 193.83, 193.20 (t, $^2J_{C-P}$ = 11.5 Hz), 188.95 (7CO), 141.62–127.22 (C-1, 3*Ph*CH_2, *Ph*$_2$CH_2CH_2*Ph*$_2$), 111.82 (d, $^2J_{C-P}$ = 7.6 Hz, C-2), 79.29, 78.11, 73.96, 75.09, 73.86, 70.92, 69.72, 69.38, 27.65 (d, $^2J_{C-P}$ = 25.3 Hz, $Ph_2CH_2CH_2Ph_2$), δ 23.64 (d, $^2J_{C-P}$ = 31.4 Hz, $Ph_2CH_2CH_2Ph_2$); ^{31}P NMR (CD_2Cl_2): δ 44.23 (d, J_{P-P} = 9.89 Hz), δ 37.55 (m, br); FAB+ mass spectrum: 1315 $[M]^+$, 1203 $[M-4CO]^+$, 1147 $[M-6CO]^+$. Anal. Calc. for $C_{60}H_{52}O_{11}P_2Ru_3$: C, 58.83; H, 3.99. Found: C, 58.86; H, 4.02%.

6. Crystallographic analysis

Yellow single-crystals of **2** suitable for diffraction analysis were grown by slow evaporation of solvent from solutions of pure compound in a diethyl ether/dichloromethane solvent mixture at −10 °C. A crystal was glued onto the end of a thin glass fiber and X-ray data were collected on a Bruker SMART APEX CCD-based diffractometer, using Mo Kα radiation (0.71073 Å) at 294 K. The raw data frames were integrated with the SAINT+ program using a narrow-frame integration algorithm [18]. Correction for the Lorentz and polarization effects were also applied by using the program SAINT. An empirical absorption correction based on the multiple

Table 4
Crystallographic data for compound **2**.

Empirical formula	$C_{59}H_{50}O_{11}P_2Ru_3$
Formula weight	1300.14
Crystal system	Orthorhombic
Lattice parameters	
a (Å)	10.2130(3)
b (Å)	23.4466(8)
c (Å)	25.6029(8)
α (°)	90
β (°)	90
γ (°)	90
V (Å^3)	6130.9(3)
Space group	$P2_12_12_1$
Z	4
Density (calculated) (mg/m^3)	1.409
Temperature (K)	294
Absorption coefficient (mm^{-1})	0.836
Crystal size (mm^3)	0.40 × 0.32 × 0.28
Theta range for data collection (°)	1.59–28.33
Index ranges	$-13 \le h \le 13$, $-31 \le k \le 31$, $-34 \le l \le 34$
Completeness to theta = 28.33°	99.8%
Absorption correction	Multi-scan from equivalents
Max. and min. transmission	1.000 and 0.889
Data/restraints/parameters	15277/4/643
Goodness-of-fit (GOF) on F^2	1.157
Final R indices [$I > 2\sigma(I)$]	$R_1 = 0.0488$, $wR_2 = 0.1364$
R indices (all data)	$R_1 = 0.0529$, $wR_2 = 0.1398$
Largest shift/error	0.001
Absolute structure parameter (Flack)	0.02(3)
Largest difference peak and hole (e$^-$ Å^{-3})	1.006 and −0.516

measurement of equivalent reflections was applied by using the program SADABS. Structure was solved by a combination of direct methods and difference Fourier syntheses and was refined by full-matrix least-square on F^2, by using the SHELXTL software package [19]. All nonhydrogens were refined with anisotropic thermal parameters. Unless indicated otherwise, the hydrogen atoms were placed in geometrically idealized positions and included as standard riding atoms during least-square refinements. Because of the disorder, one of the phenyl rings (C66–C71) had to be refined with isotropic thermal parameters. The hydride ligand H(2) was located and refined in the structural analyses using isotropic thermal parameters. The hydride ligand H(1) was located in the difference Fourier map and refined with the constraint M–H equals 1.75 Å. Crystal data, data collection parameters, and results of analysis are listed in Table 4.

6.1. Cytotoxicity in cancer cell lines

6.1.1. Cell lines and conditions

Cell lines were purchased from ATCC and cisplatin was purchased from Sigma. DU145 (prostate), MCF-7 (breast), SK-OV-3 (ovarian) cancer cells were grown in Dulbecco's Modified Eagles Medium (DMEM) and K562 (CML: chronic myelogenous leukemia), RAJI (B-cell lymphoma), MOLT-4 (ALL: T-cell acute lymphoblastic leukemia) cancer cells were grown in RPMI medium (CellGro) both supplemented with 10% fetal bovine serum (Cell Generation) and 1 unit penicillin-streptomycin (Gibco). Tissue cultures were maintained at 37 °C and humidity maintained below 90%.

6.1.2. Cytotoxicity assay

Human cancer cells were plated in twelve-well dishes at a cell density of 2.5×10^4 cells/ml/well. The cells were treated, in duplicate, 24 h later with each compound at increasing concentrations [20]. The total number of viable cells was determined after 96 h of continuous treatment by staining with trypan blue and counting number of nonstaining cells (viable) remaining in each well by using a hemacytometer. The percentage of viable cells remaining was calculated as follows: number of viable cells (compound treated)/number of viable cells (DMSO treated) * 100. Compound **1** dose response assay plot is the average percent viable cells of the treated compared to the vehicle (DMSO) treated cells. The GI_{50} (50% growth inhibition as compared to DMSO treated control) values in micromoles were determined by extrapolation from the dose response curves. Dose response curves were generated by plotting the percentage of cells at each concentration versus concentration tested. Compound **1** was chosen to produce more detailed growth curves based on overall highest activity profile. Similarly, cells were treated at increasing concentrations of cisplatin and detailed growth curves were generated. Thus the activity of compound **1** was compared to cisplatin.

Acknowledgments

This work was funded in part by PSC-CUNY Awards. RDA wishes to acknowledge the support of the USC Nanocenter. We gratefully acknowledge the help of Prof. Steven M. Graham for assistance with NMR, and the NMR facility at St. Johns University. We also thank Ronald New from mass spectrometry facility at UC, Riverside for assistance with mass spectra.

Appendix A. Supplementary material

CCDC 704003 contains the supplementary crystallographic data for this paper. These data can be obtained free of charge from The Cambridge Crystallographic Data Centre via www.ccdc.cam.ac.uk/data_request/cif. VT-^{1}H NMR in the hydride region, ^{1}H NMR, ^{13}C NMR spectra for compound **1**; ^{1}H NMR, ^{13}C NMR, ^{31}P NMR spectrum spectra **2**; ^{1}H NMR, ^{13}C NMR, ^{31}P NMR spectra for **3**; ^{1}H NMR, ^{13}C NMR, ^{31}P NMR spectra for compound **4**. Supplementary data associated with this article can be found, in the online version, at doi:10.1016/j.jorganchem.2008.11.025.

References

[1] (a) B. Rosenberg, L. VanCamp, T. Krigas, Nature 205 (1965) 698;
(b) M.C. Wani, H.L. Taylor, M.E. Wall, P. Coggon, A.T. McPhail, J. Am. Chem. Soc. 93 (1971) 2325.
[2] (a) W.H. Ang, P.J. Dyson, Eur. J. Inorg. Chem. (2006) 4003;
(b) P.J. Dyson, G. Sava, Dalton Trans. (2006) 1929;
(c) C.S. Allardyce, A. Dorcier, C. Scoloro, P.J. Dyson, Appl. Organometal. Chem. 19 (2005) 1;
(d) T.R. Johnson, B.E. Mann, J.E. Clark, R. Foresti, C.J. Green, R. Motterlini, Angew. Chem., Int. Ed. 42 (2003) 3722;
(e) A. Nguyen, A. Vessieres, P. Pigeon, M. Huche, E.A. Hillard, G. Jaouen, J. Organomet. Chem. 692 (2007) 1219;
(f) E.A. Hillard, A. Vessieres, S. Top, P. Pigeon, K. Kowalski, M. Huche, G. Jaouen, J. Organomet. Chem. 692 (2007) 13;
(g) A. Dorcier, W.H. Ang, S. Bolano, L. Gonsalvi, L. Juillerat-Jeannerat, G. Laurenczy, M. Peruzzini, A. Phillips, F. Zanoboni, P.D. Dyson, Organometallics 25 (2006) 4090.
[3] (a) R.D. Adams, B. Captain, L. Zhu, J. Am. Chem. Soc. 126 (2004) 3042;
(b) R.D. Adams, T.S. Barnhard, Z. Li, W. Wu, J. Yamamato, J. Am. Chem. Soc. 116 (1994) 9103;
(c) R.D. Adams, J. Organomet. Chem. 600 (2000) 1;
(d) V. Ferrand, G. Suss-Fink, A. Neels, H. Stoeckli-Evans, J. Chem. Soc., Dalton Trans. (1998) 3825;
(e) V. Ferrand, G. Suss-Fink, A. Neels, H. Stoeckli-Evans, Chem. Eur. J. (2003) 1046;
(f) R. Giordano, E. Sappa, J. Organomet. Chem. 448 (1993) 157;
(g) M. Castiglioni, R. Giordano, E. Sappa, J. Organomet. Chem. 491 (1995) 111.
[4] (a) E. Rosenberg, F. Spada, K. Sugden, B. Martin, L. Milone, R. Gobetto, A. Viale, J. Fiedler, J. Organomet. Chem. 668 (2003) 51;
(b) E. Rosenberg, F. Spada, K. Sugden, B. Martin, R. Gobetto, L. Milone, A. Viale, J. Organomet. Chem. 689 (2004) 4729.
[5] (a) A. Vessieres, S. Top, W. Beck, E. Hillard, G. Jaouen, Dalton Trans. (2006) 529;
(b) S. Top, E.B. Kaloun, G. Leclercq, I. Alias, M. Ourevitch, C. Deuschel, M.J. McGlinchey, G. Jaouen, ChemBioChem 4 (2003) 754;
(c) K.A. Chan, W.K. Leong, G. Jaouen, L. Leelerq, S. Top, A. Vessieres, J. Organomet. Chem. 691 (2006) 9.

[6] (a) J.E. Debreczeni, A.N. Bullock, G.E. Atilla, D.S. Williams, H. Bergman, S. Knapp, E. Meggers, Angew. Chem., Int. Ed. 45 (2006) 1580;
(b) H. Bergman, P.J. Carroll, E. Meggers, J. Am. Chem. Soc. 128 (2006) 877;
(c) L. Zhang, P. Carroll, E. Meggers, Org. Lett. 6 (2004) 521.
[7] (a) N. Sharon, H. Lis, Science 246 (1989) 227;
(b) L.A. Lasky, Science 258 (1992) 964.
[8] (a) M.L. Sinnot, Chem. Rev. 90 (1990) 1171;
(b) G. Legler, Adv. Carbohydr. Chem. Biochem. 48 (1990) 319;
(c) R.W. Franck, Bioorg. Chem. 2 (1992) 99;
(d) A.D. Elbein, Annu. Rev. Biochem. 56 (1987) 497.
[9] V.D. Reddy, J. Organomet. Chem. 691 (2006) 27.
[10] (a) V.D. Reddy, INOR # 344, 232nd ACS National Meeting, San Francisco, September 10–14, 2006.;
(b) V.D. Reddy, D. Dayal, M.V.R. Reddy, S.C. Cosenza, INOR # 687, 234th ACS National Meeting, Boston, August 19–23, 2007.
[11] M.I. Bruce, in: G. Wilkinson, F.G.A. Stone, E.W. Ebel (Eds.), Comprehensive Organometallic Chemistry, Pergamon, London, UK, 1982, pp. 843–849.
[12] (a) C. Jangala, E. Rosenberg, D. Skinner, S. Aime, L. Milone, E. Sappa, Inorg. Chem. 19 (1980) 1571;
(b) S. Aime, R. Gobetto, D. Osella, L. Milone, E. Rosenberg, Organometallics 1 (1982) 640;
(c) S. Aime, R. Gobetto, D. Osella, L. Violano, A.J. Arce, Y. Desanctis, Organometallics 10 (1991) 2854;
(d) M.A. Gallop, B.F.G. Johnson, R. Khattar, J. Lewis, P.R. Raithby, J. Organomet. Chem. 386 (1990) 121;
(e) E. Rosenberg, J. Bracker-Novak, R.W. Gellert, S. Aime, R. Gobetto, D. Osella, J. Organomet. Chem. 365 (1989) 163;
(f) S.P. Tunik, V.D. Khripoun, I.A. Balova, M.E. Borovitov, I.N. Domnin, E. Nordlander, M. Haukka, T.A. Pakkanen, D. Parrar, Organometallics 22 (2003) 3455.
[13] (a) R. Bau, M.H. Drabnis, Inorg. Chim. Acta 259 (1997) 27–50;
(b) R.G. Teller, R. Bau, Struct. Bond. 44 (1981) 1–82.
[14] H.A. Mirza, J.J. Vittal, R.J. Puddephatt, Inorg. Chem. 32 (1993) 1327.
[15] (a) J.A. Cabeza, I. Rio, V. Tiera, D. Ardura, J. Organomet. Chem. 554 (1998) 117;
(b) H.A. Mirza, J.J. Vittal, R.J. Puddephatt, Inorg. Chem. 34 (1995) 4239.
[16] S.J. Chen, K.M. Dunbar, Inorg. Chem. 29 (1990) 529.
[17] S.E. Kabir, A. Miah, K. Uddin, A.J. Deeming, J. Organomet. Chem. 476 (1994) 121.
[18] SAINT+ version 6.02a, Bruker Analytical X-ray System, Inc., Madison, Wisconsin, 1998.
[19] G.M. Sheldrick, SHELXTL, version 5.1, Bruker Analytical X-ray System, Inc., Madison, Wisconsin, 1997.
[20] (a) N.S. Reddy, M.R. Mallireddygari, S. Cosenza, K. Gummireddy, S.C. Bell, E.P. Reddy, M.V.R. Reddy, Bioorg. Med. Chem. Lett. 14 (2004) 4093;
(b) M.V.R. Reddy, M.R. Mallireddygari, S. Cosenza, V.R. Pallela, N.M. Iqbal, K.A. Robell, A.D. Kang, E.P. Reddy, J. Med. Chem. 51 (2008) 86.